IFSCC 2025 full paper (IFSCC2025-869)

"Establishment of a high cell-density suspension culture system of Adenium obesum and evaluation of the efficacy of the culture extracts"

Aimei Zhou [1], Xiaopeng Huang [1], Yan Yang [1], Qiaoxue Xiao [1], Yadong Huang [1], and Ziyi Huang [1,*]

[1] R&D Department, Tyran（Guangzhou）Biotechnology Co., Ltd., Guangzhou, China

1. Introduction

Adenium obesum, commonly known as the desert rose, is a native plant indigenous to the subsaharan region of South African countries [1-3]. Adapted to thrive under intense solar radiation in high-temperature, arid environments, these species possess remarkable moisture conservation mechanisms [4]. Beyond its ornamental value, the plant has garnered significant attention for its antioxidant, anticancer, antiviral, and immune-modulatory activities. In recent years, due to reservoirs of bioactive compounds, including triterpenoids, flavonoids, phenolic acids, and chlorogenic acid (CA) [5, 6]. For example, *Adenium obesum* leaf extract has moisturizing, emollient, and anti-aging properties. Similarly, flower extract contains a high concentration of alginate, which can reduce skin tanning and aging and effectively improve the skin's water storage function. In addition, bark extract has a strong antioxidant effect [7].

However, there are limitations to conventional propagation via seedlings or cuttings, such as slow growth rates (3-5 years to maturity) and environmental susceptibility. In addition, pathogen-related challenges such as fungal and bacterial soft rots transmitted from mother plants further limit these methods [8, 9]. Furthermore, field cultivation demands substantial land and water, raising sustainability concerns, especially in arid ecosystems [10]. These challenges emphasize the need for alternative production methods with minimized environmental impact.

Plant tissue technology has emerged as a promising solution for industrial plant-derived bioactive compounds. This approach facilitates controlled, year-round biomass production in bioreactors, independent of climatic conditions [11, 12]. Plant cell suspension cultures have enhanced secondary metabolite yield and quality in species like Schisandra and Bletilla striata Rchb.f., demonstrating commercial viability [13-16]. While *Adenium obesum* callus induction and metabolite accumulation have been explored, achieving high-density cultures with consistent bioactive content remains challenging.

This study aimed to establish an optimized high-density suspension culture system for *Adenium obesum* using plant tissue culture techniques. We focused on optimizing callus induction and refining suspension culture conditions. To maximize both biomass and enhance the accumulation of chlorogenic acid (CA). The culture system was further scaled up to the bioreactor level to evaluate its industrial feasibility. The antioxidant and pro-repair efficacy of the extracts was evaluated through vitro bioassays. The research will advance the biotechnological use of *Adenium obesum* constituents while ensuring the safety of humans and animals. This work will establish a fundamental and sustainable framework for producing plant-based cosmetic ingredients.

2. Materials and Methods

2.1 Experimental materials and callus induction

Plant Material and Explant Preparation: *Adenium obesum* (2 years old) plants were obtained commercially. All experimental procedures were performed by the research group strictly according to the ethical guidelines for plant research. Tender leaves were surface sterilized by immersion in 70% and then 5% sodium hypochlorite solution. Explants were excised into small sections (approximately 0.5 cm) for callus induction, which was carried out on Murashige and Skoog solidified medium supplemented with 0.3 mg/L naphthaleneacetic acid (NAA), 1.0 mg/L 6-benzylaminopurine (6-BA), 30 g/L sucrose, and solidified with 6.5 g/L agar (pH5.8). Cultures were maintained under a 16 h light/8 h dark photoperiod at 25±1 °C in a culture plate. Approximately 15-20 days after inoculation, callus formation was observed at the leaf margins. After 2-3 generations of successive cultures, loose and vigorously growing calluses were selected for suspension culture.

2.2 Construction of the Callus Suspension Culture System

The previously selected loose and fragile calluses (12 g FW) were transferred to an 80 mL liquid medium in a 250 mL Erlenmeyer flask for shock culture. The suspension culture medium consisted of Murashige and Skoog (MS) -based medium supplemented with 2.0 mg/L 2,4-dichlorophenoxyacetic acid (2,4-D), 0.5 mg/L 6-BA, and 30 g/L sucrose (pH 5.8). Cultures were maintained in continuous darkness at 28 ℃ with a shaker speed of 120 rpm. Subcultures were performed every 10 days, during which time large cell aggregates were removed using polypropylene filters, and turbidity was detected in the culture supernatant. The resulting cytosol was then subcultured in fresh medium at an inoculum of 1:3 (v/v) to maintain culture conditions.

2.3 Establishment of high-density suspension culture system

After 3-5 generations of subculture, stable suspension cell lines were established. To optimize high-density cultivation, we systematically evaluated two critical parameters: orbital shaking speed (T) and thidiazuron (TDZ). Four experimental groups were designed. Fresh weight measurements were recorded daily for 7 days after inoculation (n=3) to generate growth curves. Growth kinetics were analyzed using dose-response simulation modeling in GraphPad Prism 8.0.2 (GraphPad Software, Boston, MA), with model selection based on the coefficient of determination (R^2). Statistical significance was determined by two-way ANOVA followed by Duncan's multiple comparison test ($\alpha=0.05$).

2.4 Expanded culture of suspension cells and preparation of extracts

The experiments were performed in 10 L bioreactors under tightly controlled conditions, including aeration at 0.1 vvm, stirring speed of 100 rpm, and inoculation density of 20% (v/v). The culture medium was based on MS formulation supplemented with 2.0 mg/L 2,4-D, 0.5 mg/L 6-BA, 0.01 mg/L TDZ, 30 g/L sucrose, and 500 mg/L phenylalanine (a key precursor in the phenylpropanoid pathway).

Suspension cells were harvested and processed to prepare both ethanol (EtOH-ACE) and aqueous (Aqua-ACE) extracts. For Equa-ACE, cells were subjected to ethanol extraction (1:3 ratio, w/v) followed by ultrasonication for 40 min. In contrast, Aqua-ACE was prepared using ultrapure water and high-pressure homogenization (100 bar). Both extracts were centrifuged (9000 g, 10 min), and the resulting supernatants were filtered through 0.45 μm membranes.

2.5 Preparation and characterization of cell suspension extract

Chlorogenic acid (CA): The CA content in the EtOH-ACE was quantified by HPLC using a C18 column (150 × 4.6 mm, 5 μm) and a mobile phase consisting of acetonitrile (A) and 0.5% H_3PO_4 (B) at 1.0 mL/min (30 °C). The gradient elution program was set as follows: 12% A (0-2 min), 15% A (20-30 min), and 25% A (30-35 min) with detection at 327 nm. The identity of CA was confirmed by comparison of retention times and UV 327 nm with ≥98% pure reference standards. For quantification, calibration curves were generated using CA standards (6.25-100 μg/mL in 80% ethanol), showing a linear correlation (n = 3) between peak areas (Y) and concentrations (X), with results expressed as mean ± SD.

Antioxidant activity: The 1,1-diphenyl-2-picrylhydrazyl (DPPH) technique was used to test the antioxidant capacity of EtOH-ACE. The test tubes were kept in complete darkness for 30 min. Absorbance at 517 nm was measured against ascorbic acid (200 μg/mL) as a reference, and radical scavenging activity was calculated.

2.6 Evaluation of Aqua-ACE Efficacy

The functional properties of Aqua-ACE were evaluated through assays measuring collagen I expression, cell adhesion, wound healing, and antioxidant activity.

Type I collagen expression: NIH/3T3 cells were cultured in RPMI-1640 (10% FBS) and seeded in 12-well plates at a density of 2×10^5 cells per well. After cell adherence, the medium was replaced with RPMI-1640 containing 0.4% FBS and treated with test samples, DPBS (negative control), or 10 ng/mL TGF-β (positive control). The cells were then incubated at 37°C in a humidified atmosphere with 5% CO_2 for 24 hours. Subsequently, cells were harvested, total RNA was extracted, and the relative expression of collagen I was quantified by quantitative reverse transcription polymerase chain reaction (qRT -PCR).

Cell adhesion: NIH/3T3 fibroblasts (1.5×10^4 cells/well) were seeded onto 96-well plates precoated with Aque-ACE, collagen (4 mg/mL), or DPBS. After incubation for 3 h (37 ℃, 5% CO_2), adherent cells were quantified using a CCK-8 assay (450 nm absorbance).

Scratch assay: HaCaT cells (1×10^5 cells/well) were grown to 90% confluence in 12-well plates. A linear scratch was made, followed by treatment with Aque-ACE, 98 IU/mL bFGF, or DPBS. Scratch closure was monitored for 6, 24, and 48 hours.

ROS and inflammation: The ROS suppression and cell repair properties of Aqua-ACE were investigated using HaCaT. Cells were divided into control (CTRL), H_2O_2 -induced model, and treatment groups; all cultures were maintained at 37 ℃, 5% CO_2. ROS levels were assessed by flow cytometry. Inflammatory markers of IL-1α, IL-6, and TNF-α were measured by quantitative real-time polymerase chain reaction (qRT -PCR).

2.7 Statistical analysis

The means of different treatments were subjected to a two-way analysis of variance (ANOVA). SPSS software was used to evaluate the means of treatment, and significant differences were determined at $p \leq 0.05$ using Duncan's multiple range test (DMRT). Data are presented as mean ± standard error (SE).

3. Results

3.1 Callus Induction and Morphology

Primary callus formation of *Adenium obesum* was observed in leaf margin regions within 7-10 days (Fig. 1a), demonstrating a high induction frequency of over 90%. Selected callus with optimal morphological characteristics defined as bright yellow pigmentation, friable texture, and granular morphology (Fig. 1b). Subcultures were performed at 10-15 day intervals for three consecutive passages. After 3-5 subculture cycles, stabilized callus lines were obtained that exhibited improved spreading properties, accelerated proliferation rates, and maintained phenotypic stability (Fig. 1c).

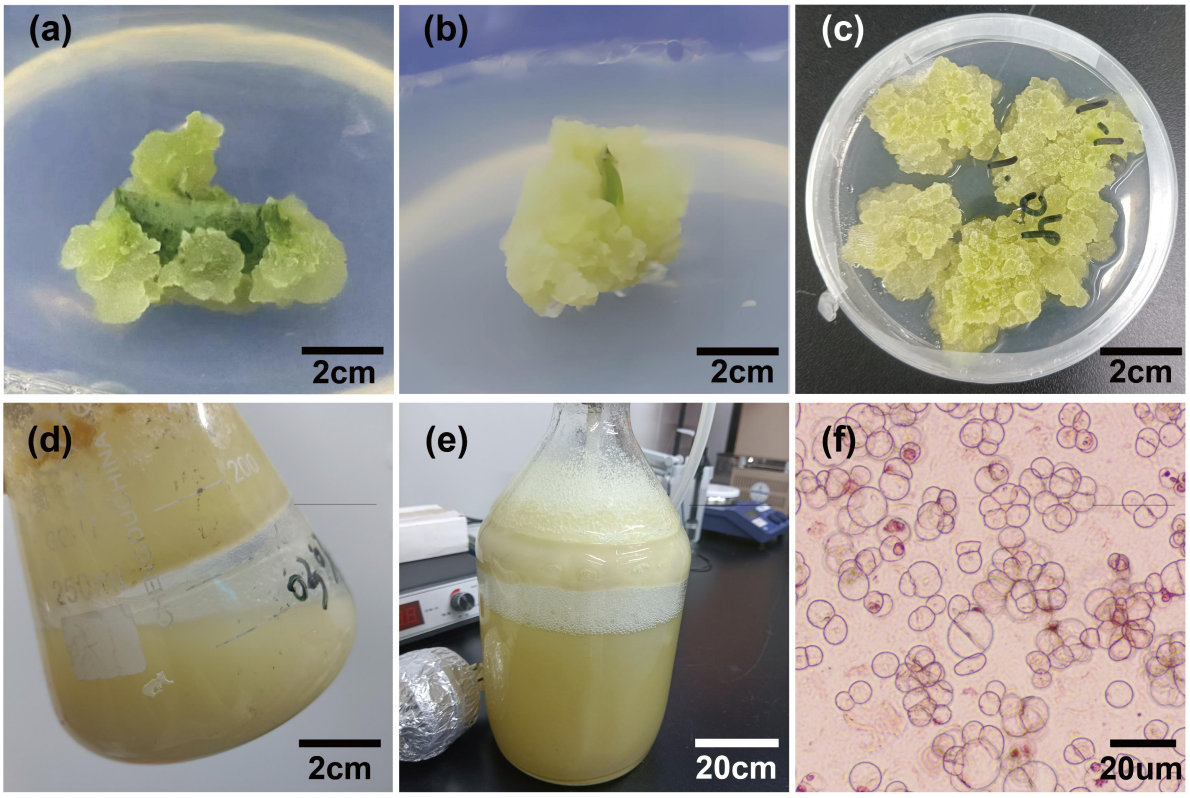

Figure 1. (a) Callus induction (initial stage); (b) Callus formation; (c) Brightly colored living callus; (d) High-density suspension culture; (e) High-density suspension culture scale-up; (f) Suspension culture cells;

3.2 Optimization of Suspension Culture Conditions

Adenium obesum callus was inoculated into a liquid MS medium and cultured under dark conditions with an initial inoculum weight of 150 g/L. After a shocked culture growth cycle of 12-15 days, the culture was subcultured to reach a final weight of 320 g/L of cellular material. Through 3-5 iterative passages at 10-day intervals, homogeneous cell populations with fine granularity, high dispersibility, chromatic uniformity, and culture clarity (medium transparency maintained at turbidity < 4 NTU) were selected. The optimized suspension system exhibited stable proliferation kinetics with characteristic cytological features: semi-translucent cytoplasm, minimal phenolic deposition, and sustained mitotic activity. Monitoring of medium turbidity confirmed metabolic stability throughout subculture phases.

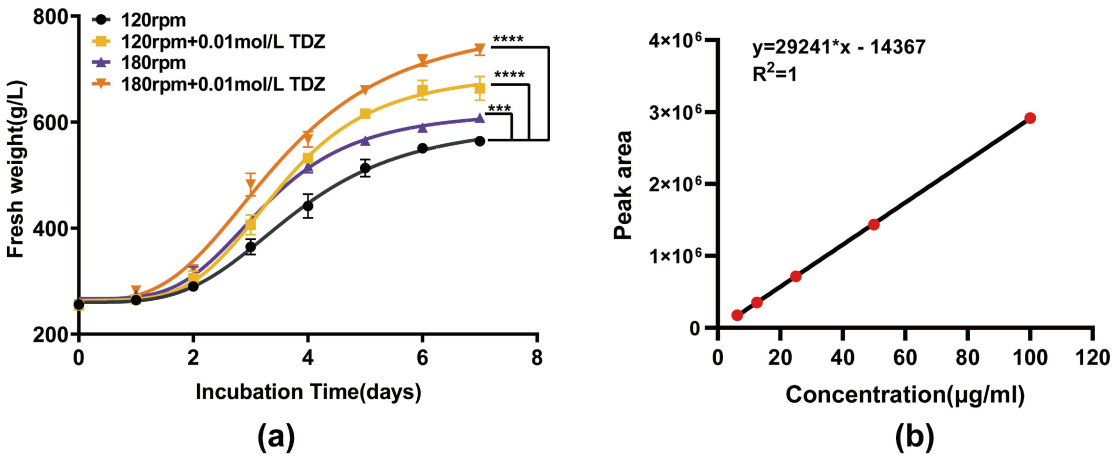

Figure 2. (a) Curve plot of the effect of rotational speed and TDZ synergy on suspension cell growth. (b) Chlorogenic acid concentration and peak area curves. Bar values with different letters indicate a significant difference (*p<0.05).

3.3 Selection and scale-up culture of high-density suspension cell lines

Longitudinal monitoring revealed time-dependent biomass accumulation influenced by stirring rate and TDZ supplementation. Growth kinetics were effectively characterized using a four-parameter logistic function ($R^2 > 0.99$). Maximum biomass was significantly increased at a stirring rate of 180 rpm in combination with 0.01 mol/L TDZ. Specifically, the maximum biomass of the 180 rpm + TDZ group increased by 21.3% (from 600.0 g/L to 790.8 g/L) compared to the control group at 120 rpm. TDZ alone increased peak biomass by 7.3% and 11.5% at 120 rpm and 180 rpm, respectively. In addition, the 180 rpm + TDZ group had the steepest growth kinetics (Hillslope = 3.188), indicating that it had the fastest rate of mesophilic biomass accumulation (Fig. 2a). LogEC50 values were shifted to the left in the TDZ-treated group, indicating earlier growth initiation. Two-way ANOVA showed significant effects of stirring rate ($F = 38.2$, $p < 0.001$), TDZ ($F = 41.7$, $p < 0.001$), and their interaction ($F = 8.3$, $p = 0.006$), indicating a synergistic mechanism.

Overall, optimizing stirring rate increased baseline biomass by 8.8%; TDZ accelerated growth and increased Hillslope by 41.2%; and their synergistic effect increased maximum biomass by 21.3%, suggesting an interaction between hydrodynamic stress and metabolic regulation.

The scale-up suspension culture using a 10 L bioreactor system exhibited a characteristic sigmoidal growth curve, with cell density reaching up to 600 g/L. *Adenium obesum* high-density suspension cell culture lines composed of single cells and small cell clusters of no more than 20 cells (Fig. 1f). Scale-up cultivation of *Adenium obesum* suspension cells was performed to enhance both biomass accumulation and secondary metabolite production.

Table 1. Four-parameter logistic model fitting results of suspension cells

Parameter	120rpm	120rpm+0.01mol/L TDZ	180rpm	180rpm+0.01mol/L TDZ
Bottom(g/L)	260.1	263.9	266.9	263.5
Top(g/L)	600.0	693.7	621.1	790.8
Hillslope	3.665	4.216	4.005	3.188
logEC50(mol/L)	0.5789	0.5472	0.5130	0.5458
R^2	0.9922	0.9936	0.9958	0.9928

3.4 Chlorogenic acid(CA)

The HPLC analysis chromatogram representing CA from EtOH-ACE ( ) showed a characteristic peak (labeled CA, tR=10.928 min, Fig. 3d). The time closely matched the retention time of the CA reference standard (tR=10.916 min, ΔtR=0.012 min, Fig. 3c). This result confirms that the suspension cells contain active secondary metabolites. The standard calibration curve showed (Fig. 2b) a strong linear correlation (y=29241x-14367, R^2=1) within the concentration range of 6.25-100 μg/mL. Quantitative analysis showed that the peak area of the target compound in the extract corresponded to a CA concentration of 31.35 μg/mL, further confirming the presence of this bioactive compound in EtOH-ACE.

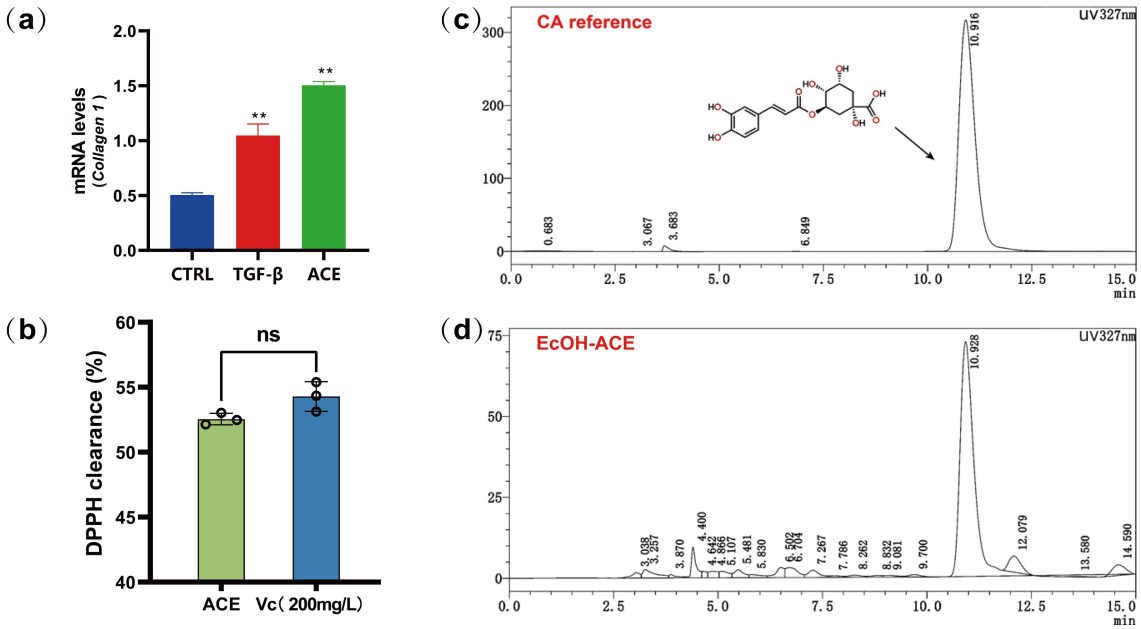

Figure 3. (a) Type I collagen mRNA expression in different treatment groups (**p<0.01 vs. control group); (b) DPPH clearance (not significant vs. Vc group). (c) HPLC chromatogram of CA stand; (d) EcOH-ACE HPLC chromatogram of CA;

3.5 Antioxidant activity

The antioxidant activity of the EtOH-ACE was evaluated using the DPPH assay. As shown in Figure 3b, the assay revealed comparable free radical scavenging capacity between ACE and the reference standard (ascorbic acid, VC) at 200 mg/mL. Quantitative analysis demonstrated similar scavenging capacities between ACE (52.55 ± 1.21%) and VC (54.29 ± 1.57%), with a marginal mean difference of 1.74% (T-test, P = 0.0696). Statistical analysis showed no significant difference (P > 0.05), indicating that ACE had comparable antioxidant activity to ascorbic acid (VC) at the concentration tested. These findings indicate that ACE could potentially be used as a natural substitute for synthetic antioxidants.

3.6 Type Ⅰ collagen expression

qPCR analysis demonstrated that collagen I mRNA levels in the control group (CTRL) were 0.5 ± 0.02. TGF-β treatment significantly increased expression to 1.0 ± 0.10 ($p < 0.01$ vs. CTRL). Notably, Aqua-ACE further elevated collagen I mRNA levels (1.5 ± 0.03, $p < 0.01$ vs. CTRL) (Fig. 3a). These results confirm that both Aque-ACE and TGF-β enhance Collagen I synthesis, with ACE showing superior efficacy.

3.7 Cell Adhesion

The cell adhesion assay evaluated the pro-adhesive activity of Aqua-ACE against NIH/3T3 fibroblasts, as shown in Figure 4b. Compared to the collagen (4 μg/mL) control, Aqua-ACE promoted cell adhesion in a concentration-dependent manner. The raw concentration of Aqua-ACE cell adhesion reached 1020.68±119.39 ($p < 0.001$), and as the concentration decreased, the cell adhesion rate decreased in a linear manner ($R^2=0.97$). Aqua-ACE outperformed the control collagen by 4.8 to 10.2 times ($p < 0.05$). The differences between 6.25% and 25% concentrations were not significant (ns) and aligned with collagen promotion.

Aqua-ACE shows that strong adhesion is likely due to bioactive compounds such as collagen and polysaccharides that mimic extracellular matrix (ECM) structures, thereby enhancing cell-matrix interactions. These findings suggest two key therapeutic potentials: first, promoting skin barrier repair through ECM regeneration; and second, mitigating age-related skin laxity by strengthening ECM integrity. With its concentration-dependent efficacy and biomimetic properties, Aqua-ACE holds promise as a dermocosmetic ingredient for skin rejuvenation and anti-laxity treatments.

3.8 Scrape wound healing assays

The enhancement of wound healing by Aqua-ACE in HaCaT cells was analyzed using a scrape wound healing, assay and compared to EGF and control (Fig. 4a, b). The result showed that Aqua-ACE demonstrated time-dependent enhancement of wound closure in HaCaT cells over 48 hours. At 6 hours, Aqua-ACE closely matched the healing rate of EGF, outperforming untreated controls by 85%. At 24 hours, it almost matched EGF while outperforming controls by 52.8% and the Aqua-ACE by 64%. At 24 hours, EGF increased migration to 61.20% ($p < 0.0001$ vs. CTRL 45.08%), while Aqua-ACE achieved 53.58% (**p=0.0067 vs. CTRL). At 48 hours, both EGF and Aqua-ACE showed wound closure: EGF at 95.06% ($p < 0.0001$ vs. CTRL 61.79%) and Aqua-ACE at 85.79% ($p < 0.0001$ vs. CTRL). The results highlight the therapeutic potential of Aqua-ACE, which mimics the reparative

effects of EGF through mechanisms involving enhanced cell migration and polarity. It has dual functionality in accelerating wound healing and supporting anti-aging.

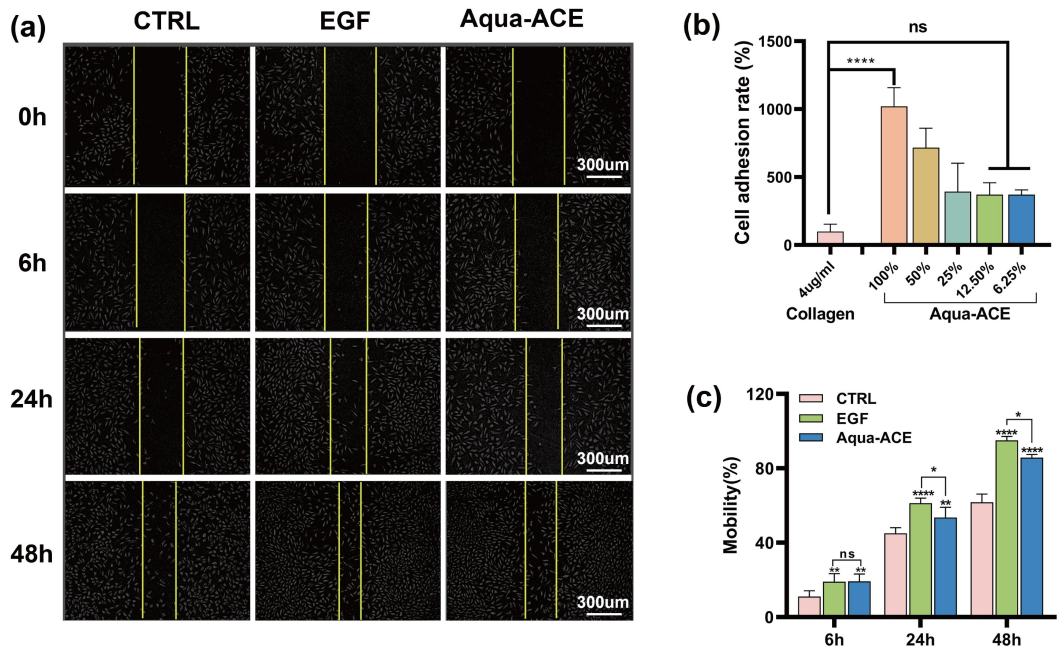

Figure 4. (a) HaCaT cells were treated with different samples at 37 ℃ for 6, 24, and 48 h, and assessing the wound healing activity was ; (b) the bar graph summarises the cell adhesion experiments and shows the percentage of adhesion for Aqua-ACE at different concentrations. (c) The bar graph summarises the wound healing experiments and shows the percentage of wound closure for Aqua-ACE and different time intervals. Data are presented as mean ± SD (n=4). Bar values with different letters indicate a significant difference (*$p < 0.05$).

3.9 Inflammatory factor levels

3.9.1 ROS level

Analysis of the data in Table 2 shows that both vitamin C (Vc) and Aqua-ACE treatments significantly reduced ROS levels compared with the model group (p = 0.0001 and 0.0004, respectively), indicating effective inhibition of ROS generation. Fluorescence analysis showed that Aqua-ACE achieved moderate ROS suppression, with values between the model and Vc groups. However, its effect was slightly less potent than vitamin C, as shown in Figure 5a.

Table 2. Inhibition rate and fluorescence intensity of each experimental group

Group	Inhibition rate	Mean	CV	SD	P value
CTRL	-	73250	1056	0.01	-
Model	-	285170	4323	0.02	-
Vc	51.26%	139000	5031	0.04	0.0001
Aqua-ACE	26.10%	210727	8932	0.04	0.0004

3.9.2 Modulation of Inflammatory Factors

As shown in Figure 5b, Aqua-ACE showed no cytotoxicity at 5%, 10%, and 20% concentrations and maintained high cell viability (97-108%). The 20% dose selected for further study significantly reduced mRNA levels of pro-inflammatory cytokines in an

inflammation model: IL-6 by 50.4% ($p < 0.01$), IL-1α and TNF-α by 59.9% each ($p < 0.001$). It also outperformed the vehicle control, which had 29.2% higher IL-6 levels ($p < 0.05$).

UV-induced skin damage triggers inflammation through the production of ROS and cytokines, including IL-1α, IL-6, and TNF-α. Aqua-ACE effectively suppressed the generation of both ROS and these cytokines, highlighting its promising therapeutic potential for combating photoaging.

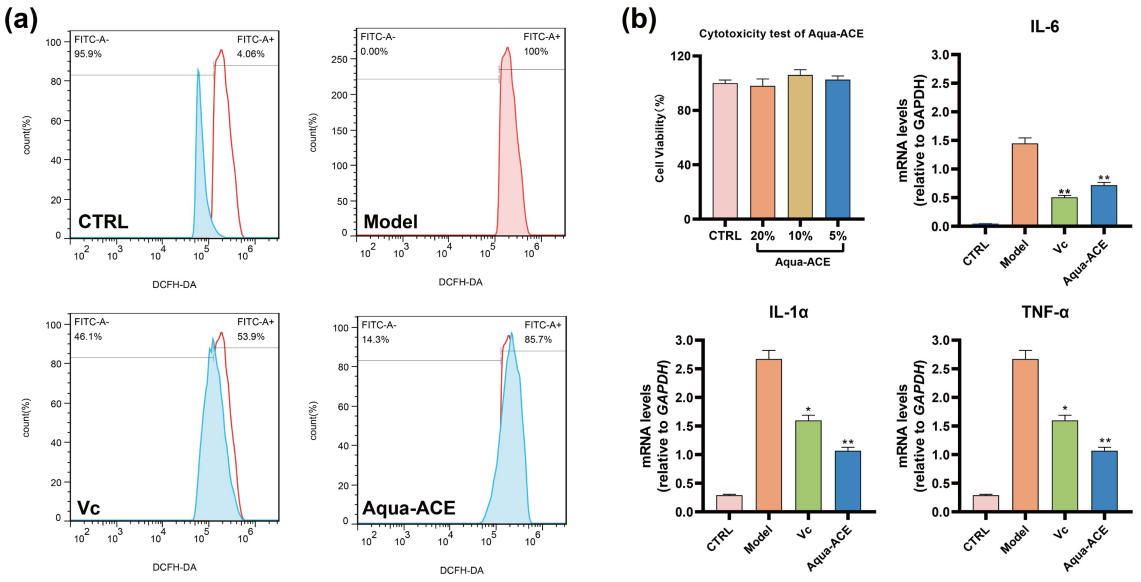

Figure 5. (a) Shows the distribution of data from flow cytometry (b) Cellularity and inflammatory factors IL-1a, IL-6, TNF-a gene levels measured. Bar values with different letters indicate a significant difference (*$p<0.05$).

4. Discussion

In this study, we successfully established a high-density suspension culture system for Adenium obesum cells, significantly surpassing the cell density limits reported in the existing literature on plant suspension cultures. By maintaining a high inoculation density, employing a relatively high agitation speed, and supplementing with cytokinin, we achieved an unprecedented biomass wet weight of up to 760 g/L, far exceeding the commonly reported cell densities, which typically range from tens to hundreds of grams per liter. Notably, in the late stages of cultivation, the cell culture medium exhibited a semi -solid paste-like state, a phenomenon rarely documented in previous studies. The application of high agitation speed, which is uncommon in conventional plant cell suspension cultures that typically maintain speeds between 50 and 120 rpm, effectively enhanced intercellular communication and nutrient exchange, thereby promoting cell proliferation. The addition of cytokinin further stimulated cell activity and division, playing a critical role in achieving such high-density culture. Furthermore, we successfully scaled up the process to a 7L bioreactor using a self-developed device, maintaining a high cell density of approximately 600 g/L, which demonstrates good scalability potential. While this scale remains modest compared to the 630 L industrial suspension culture system developed by IPPRAS [17], the clear technical pathway developed herein suggests considerable potential for further scale-up.

We evaluated the molecular, biochemical, and bioactive properties of cell suspension extracts. The results showed that ACE extracts were rich in chlorogenic acid and exhibited strong antioxidant capacity, alongside significant wound healing and anti-photoaging effects. Notably, ACE treatment increased collagen I gene expression and enhanced cell adhesion, suggesting that the adhesion-promoting effect of ACE may be mediated by polysaccharide-mediated matrix anchoring in conjunction with increased collagen I expression. Supporting these molecular and biochemical findings, scratch wound healing assays further confirmed the beneficial effect of ACE treatment on skin cell function. Additionally, the extracts effectively modulated reactive oxygen species (ROS) and reduced pro-inflammatory cytokines, thereby mitigating inflammation and oxidative damage induced by photoaging in skin cells. Taken together, these results highlight the potential of ACE as a functional ingredient for skin care applications.

Given the scarcity of studies on *Adenium obesum* suspension culture studies, our work fills a critical gap and lays the foundation for the future development of high-density plant cell cultures. Beyond efficient secondary metabolite production, this system offers a promising animal-component-free eukaryotic platform for recombinant protein expression and supports conservation efforts for endangered plants, thereby bridging biotechnology and biodiversity preservation.

5. Conclusion

This study established a high-density suspension culture system for *Adenium obesum* with biomass reaching 760 g/L, far beyond typical plant cell cultures. Key factors include high inoculation density, increased agitation speed, and cytokinin addition.

The extract from these cells shows strong antioxidant, wound-healing, and anti-photoaging properties, making it a promising ingredient for skin care products. The culture system was successfully scaled up to 7 L, showing good potential for further industrial expansion.

Our platform not only provides a sustainable source of valuable plant metabolites but also offers an animal-component-free system for recombinant protein production and aids plant conservation efforts. Overall, this research lays a solid foundation for large-scale production and diversified applications of desert rose cells, combining biotechnological innovation with biodiversity protection.

Reference

1. Ahmed SK, Versiani MA, Ikram A, Sattar SA, Faizi S. Cytotoxic cardiac glycosides from the fruit (pods) of *adenium obesum* (forssk.) roem. & schult. Natural Product Research. 2017;31:1205-8.

2. Gurung AB, Ali MA, Lee J, Al-Hemaid F, Farah MA, Al-Anazi KM. Molecular docking elucidates the plausible mechanisms underlying the anticancer properties of acetyldigitoxigenin from a*denium obesum*. Saudi Journal of Biological Sciences. 2020;27:1907-11.

3. Colombo RC, Da Cruz MA, Carvalho DU, Hoshino RT, Alves GAC, De Faria RT. *Adenium obesum* as a new potted flower: growth management. OH. 2018;24:197-205.

4. Araújo RC, Rodrigues FA, Dória J, Pasqual M. In vitro germination of *adenium obesum* under the effects of culture medium and light emitting diodes of different colors. Plant Cell Tiss Organ Cult. 2022;149:523-33.
5. Hossain MdA. A review on *Adenium obesum*: A potential endemic medicinal plant in Oman. Beni-Suef University Journal of Basic and Applied Sciences. 2018;7:559-63.
6. Tatsuzawa F, Yoshikoshi A, Takehara A, Suzuki S. Flavonoids from the flowers o*f Adenium obesum* (Forssk.) Roem. & Schult., Mandevilla sanderi (Hemsl.) Woodson, and Nerium oleander L. (Apocynaceae). Biochemical Systematics and Ecology. 2021;99:104347.
7. Suleiman MHA, Brima EI. Phytochemicals, Trace Element Contents, and Antioxidant Activities of Bark of Taleh (Acacia seyal) and Desert Rose (*Adenium obesum*). Biol Trace Elem Res. 2021; 199: 3135-46.
8. Pinto Junior FF, Ribeiro BDSB, Sousa LAMD, Silva FLDS, Silva KRC, Moraes LF, et al. Uso de extrato de pitanga no controle de fungo fitopatogênico em *adenium obesum*. RSD. 2022;11:e135111335335.
9. Roy K, Fatmi U. Impact of grafting techniques on success rate, survival and growth of different adenium (*adenium obesum*) scions under prayagraj agro-climatic conditions. IJPSS. 2022;1677-83.
10. Yamauchi T, Abe F. Cardiac glycosides and pregnanes from *adenium obesum* (studies on the constituents of adenium. I). Chemical & Pharmaceutical Bulletin. 1990; 38: 669.
11. Kong EYY, Biddle J, Kalaipandian S, Adkins SW. Coconut callus initiation for cell suspension culture. Plants. 2023; 12: 968.
12. Taghizadeh M, Nasibi F, Kalantari KM, Benakashani F. Callogenesis optimization and cell suspension culture establishment of dracocephalum polychaetum bornm. and dracocephalum kotschyi boiss.: An in vitro approach for secondary metabolite production. South African Journal of Botany. 2020; 132: 79-86.
13. Guru A, Dwivedi P, Kaur P, Pandey DK. Exploring the role of elicitors in enhancing medicinal values of plants under in vitro condition. South African Journal of Botany. 2022;149:1029-43.
14. Abdulhafiz F, Mohammed A, Reduan MFH, Kari ZA, Wei LS, Goh KW. Plant cell culture technologies: A promising alternatives to produce high-value secondary metabolites. Arabian Journal of Chemistry. 2022;15:104161.
15. Zhou Y-Q, Li T-C, Cheng Y-P. Production of Schisandrin A and Schisandrin B from Callus and Suspension Cell Cultures of *Schisandra chinensis*. Natural Product Communications. 2017;12(6) :937-940.
16. Pan Y, Li L, Xiao S, Chen Z, Sarsaiya S, Zhang S, et al. Callus growth kinetics and accumulation of secondary metabolites of Bletilla striata Rchb.f. using a callus suspension culture. Chen J-T, editor. PLoS ONE. 2020;15: e0220084.
17. Titova M, Popova E, Nosov A. Bioreactor systems for plant cell cultivation at the institute of plant physiology of the russian academy of sciences: 50 years of technology evolution from laboratory to industrial implications. Plants. 2024; 13: 430.